Available online at www.sciencedirect.com
SCIENCE DIRECT®
Journal of Nuclear Materials 336 (2005) 81–89
journal of nuclear materials
www.elsevier.com/locate/jnucmat

Ion-induced amorphization in ceramic materials

G. Szenes *

Department of General Physics, Eötvös University, 1518 Budapest, P.O. Box 32, Hungary

Received 3 June 2004; accepted 10 September 2004

Abstract

Amorphization induced by swift heavy ions is discussed, the main features are reviewed and explained by the author's model. In Al_2O_3 and $MgAl_2O_4$ the recrystallization reduces considerably the track diameters. The threshold electronic stopping power for amorphization S_{et} can be estimated reliably for these solids from the position of the amorphous–crystalline boundary formed at high ion fluences. The results are in good agreement with the predictions of the model. Experiments on CeO_2 and UO_2 are discussed. Estimates of S_{et} are made for β-Si_3N_4, CeO_2, pure ZrO_2, $ZrSiO_4$, and UO_2, and $10.1 > S_{et} > 6.2$ keV/nm is obtained at room temperature for fission fragment energies. At about 1000 °C operation temperature, S_{et} is reduced by about 35–50%. No amorphization is expected by ion bombardment in AlN, SiC (semiconductors) and MgO (ionic crystal).

1. Introduction

Recently, a growing activity is observed in the research of ceramic materials for inert matrices. An important requirement is the stability of the proposed ceramics against the impact of fission fragments (ff), which can induce tracks (amorphous, recrystallized) and swelling. Simultaneously, high stresses can evolve, which affect the mechanical stability. Irradiation with high fluences may induce complete amorphization. In insulators, the threshold electronic stopping power for track formation S_{et} is the main parameter characterizing the amorphization. In this paper, after a brief review of track formation in ion irradiation experiments, we present theoretical estimates of S_{et} in various ceramics and compare them with the available experimental data.

* Tel.: +36 1 372 2821; fax: +36 1 372 2811.
E-mail address: szenes@ludens.elte.hu

2. Ion-induced tracks in solids

2.1. Common features

The kinetic energy of energetic ions in a solid is transferred predominantly to the electron system. This type of energy loss is characterized by the electronic stopping power S_e. If the energy deposition from the excited electron system to the lattice is strongly localized, often tracks are formed in the target. An ideal ion track is an amorphous cylinder in a crystalline matrix with the radius R_e. Such structures have been observed in many irradiated solids, mostly in insulators [1].

Close similarities exist between the track evolution curves in various insulators. We found that $dR_e^2/d\ln S_e = a^2(0) = 20\,\mathrm{nm}^2$ ($R_e < a(0)$) for a number of track forming insulators. This is demonstrated by the track data of TeO_2 and $Y_3Fe_5O_{12}$ in Fig. 1. The plots show that the initial slope of the track evolution curves does not depend on the ion energy and on the target material. The data were obtained in experiments with

0022-3115/$ - see front matter © 2004 Elsevier B.V. All rights reserved.
doi:10.1016/j.jnucmat.2004.09.004

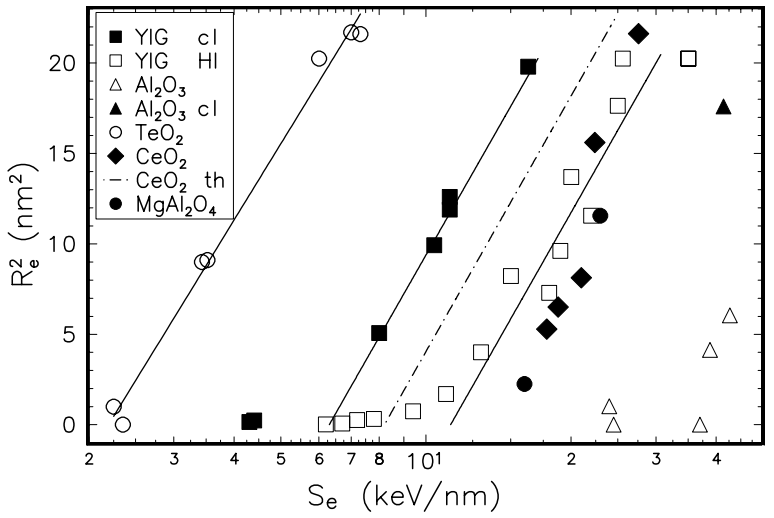

Fig. 1. Variation of the track size (R_e track radius) with the electronic stopping power S_e in various solids for $E < 2.2$ MeV/nucleon except $Y_3Fe_5O_{12}$ for which data for $E > 8$ MeV/nucleon are also shown (YIG (HI)). In the legend cl stands for irradiation with C_n carbon cluster ions. The dashed line is a theoretical curve for CeO_2 (th) according to Eqs. (1) and (3). For details see Refs. [2–5,7].

high-energy ions ($Y_3Fe_5O_{12}$, $7.6 < E < 20$ MeV/nucleon [2,3]), low-energy ions (TeO_2, $0.6 < E < 2.3$ MeV/nucleon [4]) and C_n carbon cluster ions ($Y_3Fe_5O_{12}$, $E < 0.15$ MeV/nucleon [5]). Tracks measured in Al_2O_3, $MgAl_2O_4$, and CeO_2 are also shown in the figure and the deviations from the 'regular' behavior will be discussed later.

We found a simple linear relationship between the S_{et} values and the term $\rho c T_o$ [6], where ρ, c, T_m and T_{ir} are the density, average specific heat for the temperature range of the spike, the melting point and the irradiation temperature, respectively, and $T_o = T_m - T_{ir}$. This is a strong evidence in favor of the thermal spike origin of track formation. As an approximation, the Dulong–Petit rule is applied to estimate the values of c.

2.2. Thermal spike model

We elaborated a simple model which accounts for various thermal spike effects in ion–solid interaction including track formation [6]. We assumed that (i) a thermal spike is induced along the ion trajectory; (ii) a radial Gaussian temperature distribution is a good approximation for the ion-induced temperature increase during cooling; (iii) the track radius is equal to the maximum melt radius. We derived the following simple equations

$$R_e^2 = a^2(0)\ln(S_e/S_{et}) \quad \text{for } S_e < 2.7S_{et}, \tag{1}$$

$$R_e^2 = \frac{a^2(0)S_e}{2.7S_{et}} \quad \text{for } S_e > 2.7S_{et}, \tag{2}$$

$$S_{et} = \frac{\pi \rho c T_o a^2(0)}{g}, \tag{3}$$

where gS_e is the fraction of the deposited energy transferred to the thermal spike and $a(0) = 4.5$ nm characterizes the initial width of the temperature distribution in the spike [6]. Eqs. (1) and (2) describe the track evolution and Eq. (3) is the condition for the formation of ion-induced melt. We note that the efficiency g in insulators varies with the specific ion energy E and $g = 0.17$ for $E > 8$ MeV/nucleon (high velocity range) and $g = 0.4$ for $E < 2.2$ MeV/nucleon [7] (low velocity range). Thus the model has no free parameters in the low and high velocity ranges. The spike thermal energy gS_e varies in our model with E for S_e = constant and the initial width of the spike is $a(0)$ = constant. This concept has been successfully used in various applications [8–10]. In the thermal spike model of Toulemonde et al. the width of the spike varies with E and its energy is constant ($g = 1$ in our notation). However, this model cannot explain the typical uniform behavior shown in Fig. 1 for TeO_2 and YIG and the linear variation of S_{et} with $\rho c T_o$ [2,3,11,12].

We remind the reader that Eqs. (1)–(3) do not take into account recrystallization, and R_e is the possible maximum radius of the track which can be reduced or completely diminished as a result of the response of the target material. When Eqs. (1)–(3) are combined the model predicts an $R_e^2 - S_e/\rho c T_o$ scaling for experiments with similar ion velocities. The normalized track evolution curves are shown in the low velocity range for $R_e > a(0)$ in Fig. 2. The experimental data include those obtained by irradiation with monoatomic and cluster ions as well [4]. The scaling is well fulfilled for

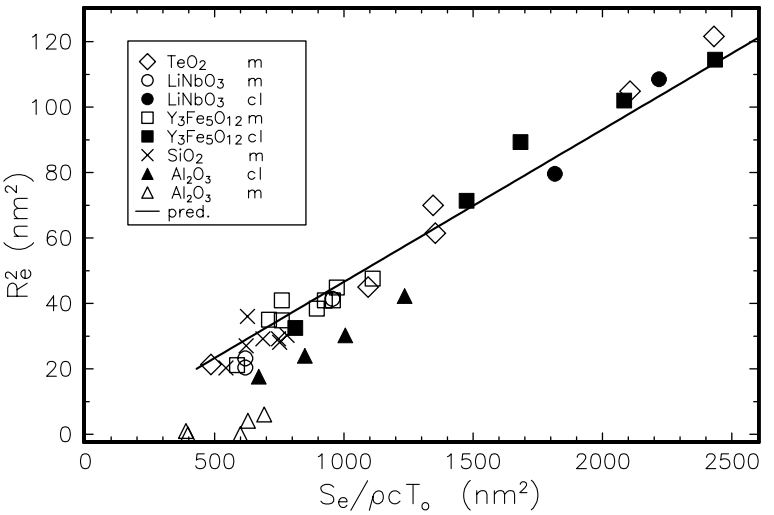

Fig. 2. Variation of the track size (R_e track radius) with the electronic stopping power S_e for irradiation with low velocity ions ($E < 2.2$ MeV/nucleon). In the scaling term ρ, c are the density, average specific heat, respectively, and $T_o = T_m - T_{ir}$ where T_m is the melting point and T_{ir} is the irradiation temperature. In the legend m and cl denote irradiations with monoatomic and C_n carbon cluster beams. The full line is drawn with the slope $m = g/2.7\pi$ (see Eqs. (2) and (3)). For details see Refs. [4,7,8].

$Y_3Fe_5O_{12}$, $LiNbO_3$, TeO_2 and SiO_2 (other data sets have not been reported till now). Considerable track recrystallization distorts the scaling, and deviations from the master curve occur. Therefore, the successful scaling means that the reduction of the track radius is negligible for these materials. Our model can predict R_e and S_{et} for these solids with uncertainties comparable to the experimental error in those energy ranges ($E < 2.2$ MeV/nucleon and $E > 8$ MeV/nucleon), where the efficiency g is reliably known [7].

In the following, the experiments on ceramics Al_2O_3, $MgAl_2O_4$, CeO_2 and UO_2 are reviewed for which the deviations from the 'regular' behavior are considerable. Our aim is to estimate S_{et} from the experiments since the damage is strongly reduced for $S_e < S_{et}$. We cannot use Eqs. (1) and (2) for this purpose, because the measured track sizes strongly depend on the experimental conditions and the kinetic parameters of the process may control the final state of the irradiated crystals. In this case instead of the analysis of individual tracks, irradiations with high fluences are useful, when an amorphous–crystalline interface is formed as a result of track overlapping. In such experiments the results are less affected by the kinetic parameters, therefore, a reliable estimate of S_{et} can be made from the position (depth) of the interface. We analyze this method in detail as it is a new procedure.

2.3. $MgAl_2O_4$

Ion-induced tracks were reported in Refs. [13–16] applying I, Kr, Xe, Pb, U and C_{60} carbon cluster beams. The track diameters vary scarcely for irradiation with high velocity ions. A smooth curve through these data points crosses the S_e axis at a value which is lower than the crossing point for low velocity data [13]. Just the opposite is expected, as the irradiation with low velocity ions is more efficient for the formation of tracks (see Fig. 1). Therefore, the large differences between the track sizes cannot be explained by the velocity effect alone [2]. No amorphous tracks were observed by transmission electron microscopy (TEM). It was proposed that amorphous spinel could be easily recrystallized by the 100–200 keV electron beam and this might strongly affect the result of TEM studies [15]. Tracks induced in $MgAl_2O_4$ only by low velocity ions are shown in Fig. 1. According to Eqs. (1) and (3) the theoretical curve would cross the axis at $S_e = 9.3$ keV/nm.

High fluence I irradiations were performed with 70 MeV and 85 MeV energy by Wiss et al. [13] and Aruga et al. [17], respectively, and the depth of the amorphous–crystalline interface d_{am} and the heights of the ion-induced surface steps z were determined relative to a masked part. Aruga et al. observed $d_{am} = 6$ μm at $\Phi t = 1.2 \times 10^{19}$ ions/m^2 and $z \approx 1$ μm, however z had a maximum of about 2 μm at the boundary. Wiss et al. studied amorphization at various fluences up to $\Phi t = 5 \times 10^{19}$ ions/m^2, and they derived the swelling as $s = z/d_{am}$. They found $d_{am} = 5$ μm and $s = 0.33$ for irradiation at room temperature with $\Phi t = 5 \times 10^{19}$ ions/m^2. The electronic stopping power S_{ei} was estimated at the amorphous–crystalline interface and 4 and 6 keV/nm were obtained by Aruga et al. and Wiss et al., respectively. These values were considered as estimates

of S_{et}. The formation of the amorphous–crystalline interface proves that the tracks are at least partially amorphous and amorphization is possible only above a critical value $S_e > S_{ei}$. Unexpectedly, S_{ei} were much lower than S_{et} estimated from Eq. (3).

We propose a slight correction to the above analysis. The swelling is accompanied by a reduction of the density in the irradiated layer. S_{ei} was calculated in Refs. [13,17] neglecting the change in the density of the irradiated layer. However, the energy loss of the projectile is lower in the amorphous layer than it would be in a crystal of the same thickness, because of the lower density. Therefore S_{ei} was underestimated in Refs. [13,17]. We found that the original thickness of the amorphized layer was $d = d_{am}(1-s) = 3.33$ μm in the experiment of Wiss et al. [13] and $S_{ei} = 9.15$ keV/nm at this depth according to the SRIM code [18]. We note that it is reasonable to characterize the swelling with $s' = z/d = s/(s-1)$ instead of $s = z/d_{am}$ used in Ref. [13]. With this correction the swelling of the spinel $s' = 0.5$ at $\Phi t = 5 \times 10^{19}$ ions/m^2, which is considerably higher than $s = 0.33$ reported by Wiss et al. [13]. We also made an estimate based on the experiment of Aruga et al. Because of some uncertainty in the correct value of z we made use of the swelling measurements in Ref. [13]. We obtained $s = 0.26$ and $z = 1.56$ μm for $\Phi t = 1.2 \times 10^{19}$ ions/m^2, which agrees well with the average step height $z = 1.5$ μm measured in the experiment. With this value, $d = 4.44$ μm and $S_{ei} = 8.6$ keV/nm. This method is rather sensitive to the accuracy of d: a change of the thickness by 0.1 μm corresponds to a shift of S_{ei} by about 0.25 keV/nm. Eq. (3) provides $S_{et} = 9.3$ keV/nm for $MgAl_2O_4$. The good agreement between S_{ei} and S_{et} is an indication that amorphization is linked to the melt formation in both cases. Therefore, the correct value of S_{ei} can be used as a good experimental estimate of S_{et}.

There is no direct evidence that the ion-induced tracks or the track cores are amorphous in $MgAl_2O_4$. Nevertheless, complete amorphization has been achieved by irradiations with high fluences. Zinkle et al. [16] performed experiments with 72 MeV I ions up to the fluence $\Phi t = 1 \times 10^{20}$ ions/m^2. They found that first a metastable crystalline phase was formed at $\Phi t < 1 \times 10^{19}$ ions/m^2 and further irradiation lead to amorphization. On the other hand Aruga et al. observed complete amorphization at $\Phi t = 1.2 \times 10^{19}$ ions/m^2 in an experiment with the same beam parameters [17]. Wiss et al. did not report about this intermediate crystalline phase either and they observed that the swelling varied smoothly in the range of $1 \times 10^{18} - 1 \times 10^{21}$ ions/m^2 [14]. In our theoretical estimate we use the ρ, c and T_m values of the spinel. If amorphization proceeds through an intermediate crystalline phase, different values ought to be used. The reasonable agreement between the predicted and experimental values of S_{et} indicates that if the intermediate phase exists its physical parameters are close to those of the spinel.

2.4. Al_2O_3

Results on ion-induced tracks were reported by Canut et al. [19,20] and Ramos et al. [21]. Sapphire single crystals were irradiated by Pb and U ions of $E = 0.4$–3.5 MeV/nucleon specific energy in Refs. [19,20], and the track diameters were determined from Rutherford backscattering in channeling geometry (c-RBS). In Ref. [21] fullerene ions of 10–30 MeV energy were used and the track diameters were measured by TEM and high resolution electron microscopy (HREM). The results for $E < 2.2$ MeV/nucleon are shown in Figs. 1 and 2.

In these experiments: (i) the tracks quickly recrystallized in the electron microscope during HREM measurements; (ii) the track diameters were rather different at nearly equal values of S_e; (iii) $S_{et} \approx 18$–21 keV/nm was obtained from the track evolution curves for low velocity ions [20,21]. The results under (i) and (ii) indicate that kinetic factors are important in the formation of the final diameter of tracks. For this reason we do not consider (iii) as a reliable estimate. Previously, (ii) was attributed to the more efficient track formation by low velocity C_{60} ions (velocity effect) [21]. However, we do not agree with this as the tracks induced in YIG and $LiNbO_3$ by (low velocity) monoatomic and cluster beams scale in Fig. 2 in contrast to the case of Al_2O_3. In Figs. 1 and 2 the track data of Al_2O_3 are shifted with respect of the theoretical curves indicating a considerable reduction of R_e. The relative reduction is higher at small track radii and this seems to be valid for $MgAl_2O_4$ and CeO_2 as well. Similarly to $MgAl_2O_4$, the estimation of S_{et} from the track size seems to be unreliable.

Recently Aruga et al. irradiated sintered alumina with iodine ions of 0.67 MeV/nucleon initial energy and measured the depth of the amorphization front from the surface d_{am} at various fluences in the range of $1.2 - 12 \times 10^{18}$ ions/m^2. At the highest fluence they found $d_{am} = 4.5$ μm and an average surface step of $z = 0.65$ μm [22], which were related to the amorphization [17]. They estimated $S_{ei} \approx 4$–5 keV/nm at the amorphous–crystalline phase boundary and took this value for S_{et} [17,22]. This is much lower than S_{et} derived from the track evolution [20,21].

In the analysis of Aruga et al. the density reduction in the amorphous phase was neglected again. We took this into account as in the case of $MgAl_2O_4$. We obtained $d = 3.85$ μm and $S_{ei} = 9.9$ keV/nm at the phase boundary, which is in good agreement with our theoretical prediction $S_{et} = 9.8$ keV/nm based on Eq. (3). According to (iii) no amorphization could be induced by the 85 MeV iodine beam in the experiment of Aruga et al., as $S_e = 18.7$ keV/nm at the surface. This contradiction confirms again, that the extrapolations may lead to

incorrect results when they are based on the parameters of individual tracks.

The good agreement between the corrected experimental S_{ei} and the theoretical S_{et} values indicates that the formation of the amorphous–crystalline interface is closely related to the formation of the ion-induced melt. There are several other ion-induced effects, which are also related to S_{et}. We showed that the heights of ion-induced hillocks h on the surface of mica are proportional to the spike thermal energy and they occur at $S_e > 2.7\,S_{et}$ [10]. In this case, the melt is extruded above the surface due to thermal stresses. Recently, the variation of h with S_e was measured on sapphire by atomic force microscopy (AFM) [21,23]. We deduced S_{et} from the analysis and found good agreement with Eq. (3) [24]. In inelastic mixing the interdiffusion through an interface is considerably accelerated when an ion-induced melt is formed. Bolse et al. concluded that Eq. (3) is in good agreement with the values of S_{et} deduced from the mixing experiments for various materials including sapphire as well [25]. Thus it is supported by several independent experiments that Eq. (3) provides a correct estimate of S_{et} for sapphire.

The experiments described in Refs. [17,19–25] justified the validity of Eq. (3) in sapphire with the g and $a(0)$ values typical for insulators. Thus the non-standard behavior of tracks in sapphire is not due to an anomaly in the formation of the melt. In our model we assumed that the amorphous volume is proportional to the maximum volume of the melt. We found that the proportionality factor is $k = 1$ for those solids for which the scaling is valid [6]. However, in sapphire $k < 1$ and $k \neq$ constant. Thus a smaller track is formed from the melt which we attribute to partial recrystallization.

The interface method may be suitable for the estimate of S_{et} even if only a few percent of small tracks are stable against complete recrystallization. The lower the fraction of 'stable' tracks, the higher the fluence to form the boundary. If only tracks with $R \geqslant 1.5$ nm are stable against complete recrystallization, S_{et} deduced from the depth of the boundary is about 10% higher than the value without recrystallization. The good agreement between the experimental and theoretical values of S_{et} indicates that a fraction of tracks with $R_e \leqslant 1.5$ nm probably survive recrystallization in Al_2O_3. The extent of recrystallization may depend on the beam (ion or electron) load during the measurements, i.e. it may be related to the applied experimental method. This may be the reason of the large scatter of track data. According to our estimate for the TEM studies of Ramos et al. [21], the reduction of the track diameters is 15–25% compared to the value calculated by applying Eq. (2) with $S_{et} = 9.8$ keV/nm.

2.5. UO_2

In spite of its practical importance no systematic studies have been reported on the response of UO_2 to irradiation by swift heavy ions. Ion-induced tracks were directly observed by AFM after irradiation with 1 GeV Pb ions [26]. Recently, Garrido et al. studied the changes in the c-RBS spectra after irradiation with 340 MeV Xe ions. The spectra did not show considerable randomization after irradiation with high ion fluences [27]. The results were explained by assuming that the tracks were not amorphous, but crystalline with small misorientation relative to the matrix. On the other hand, the track formation in UO_2 has been successfully studied by TEM by Wiss et al. [28]. The diameters were in good agreement with the predictions of our model applying the same thermal spike parameters as for other insulators: tracks with radii 4.8 nm and 4.4 nm were measured after U irradiations with 1300 MeV and 2713 MeV, while our theoretical estimates were 4.64 nm and 4.52 nm, respectively, without any fitting parameter. The agreement between the predicted and the experimental track radii indicate that the localization of the energy deposition in UO_2 is similar to that in other insulators. The contradiction of the c-RBS and the TEM results may arise from the different sensitivity of the two methods to small misorientation of grains: the tracks can be clearly visible by TEM, while no randomization is observed by c-RBS. We consider the inclination of UO_2 to recrystallization as the main difference in the behavior of UO_2 and other insulators.

Our model can estimate the radii of the cylinders around the projectile, where the structure of UO_2 is modified. By applying Eq. (3), our prediction for room temperature irradiation is $S_{et} = 8.6$ keV/nm for typical fission energies. An estimate of the experimental value can be deduced applying Eqs. (1) and (2) to the two track data. This leads to a mean value $S_{et} = 20.4$ keV/nm for irradiations with high velocity ions ($g = 0.17$) which corresponds to $S_{et} = 8.66$ keV/nm for fission fragments ($g = 0.4$). The excellent agreement between the experimental and theoretical values should not be overrated again since only two tracks could be used for the evaluation. Besides the irradiations with U ions, Wiss et al. reported on experiments with Xe ions of $E = 1.3$ MeV/nucleon energy ($S_e = 29$ keV/nm). R_e was measured after annealing at 900 °C for Xe irradiation [28]. In experiments with ^{127}I ions of $E = 0.6$ MeV/nucleon energy the samples were preirradiated with Kr ions and the irradiations were performed above room temperature [29]. Our opinion is that the experiments with Xe and I beams are not suitable for establishing reliably S_{et} because of the non-standard sample conditions. Nevertheless, 22–29 keV/nm was deduced for the threshold for track formation. However, it was not specified for which velocity range was this valid [29]. If this estimate is valid for high ion velocities, then it is not far from ours.

Recently, information was also published about extensive irradiation experiments with Pb, Au, and Xe beams in GSI (Darmstadt, Germany) with Xe, Sn and C_{60} beams in the HMI (Berlin, Germany), GANIL

(Caen, France) and in IPNO (Orsay, France), respectively [29]. Although $S_e > 29$ keV/nm was in these experiments, no track data have been published yet. The new data may be useful in checking the estimates for S_{et}.

2.6. CeO_2

This material is also a candidate for inert matrices. To simulate the effect of fission products CeO_2 samples were irradiated by I and Xe ions in the range of 70–210 MeV [30,31]. The track diameters were measured by TEM. The results are shown in Fig. 1 and they are similar to those obtained for Al_2O_3 and $MgAl_2O_4$. The tracks are considerably smaller than expected according to Eqs. (1)–(3) and the relative deviations from the theoretical line (dashed line in Fig. 1) increase with the reduction of S_e. Thus while the deviation of the diameters for 210 and 100 MeV Xe ions are 7% and 12%, respectively, it is more than 40% for 70 MeV I irradiation. No information is available about high-fluence measurements. Nevertheless, it is reasonable to assume that the small track size is the result of recrystallization and Eq. (3) provides a good estimate ($S_{et} = 8.2$ keV/nm) for the onset of track formation.

2.7. $ZrSiO_4$

This material melts incongruently at $T_{im} = 1960$ K [32]. The crystalline structure becomes unstable at $T > T_{im}$. There is no time for a long-range phase separation because of the very fast heating and cooling. However, the local structure is destroyed. Thus T_{im} can be applied in Eq. (3) for the temperature and we obtain $S_{et} = 14.5$ keV/nm for high ion velocities. Bursill and Braunshausen irradiated $ZrSiO_4$ samples by Pb ions of 14 MeV/nucleon energy [33]. They performed TEM and HREM measurements and observed ion-induced tracks. They measured $R_e = 4$ nm for track radii with an error below 5%. Our estimate is $R_e = 4.18$ nm by using Eq. (1). The good agreement between the measured track radius and our estimate justifies again the reliability of our predictions.

3. General remarks

The estimates of S_{et} in Fig. 3 from track evolution curves for $E < 2.2$ MeV/nucleon are completed with the results of the present study. The results for Al_2O_3, $MgAl_2O_4$ and UO_2 nicely fit to the general linear dependence predicted by Eq. (3). We believe that Eq. (3) provide a reliable estimate for insulators. The plots in Figs. 1 and 3 prove that the $a(0)$ and the g parameters have common values in insulators including Al_2O_3, $MgAl_2O_4$ and UO_2. We note that $a(0)$ and g are parameters characterizing the spike. The uniformity of these parameters in insulators means that the energy distribution in the thermal spike is identical in these solids for a given S_e.

We note that Fig. 2 is valid for room temperature irradiations. However, the operating temperatures of inert matrices may be up to 1000 °C. The reduction of S_{et} at high temperatures can be estimated by applying Eq. (3). One can get a first estimate by multiplying the room temperature value by $(T_m - 1300)/(T_m - 300)$ (T_m in K). This corresponds to about 50% reduction of S_{et} for Al_2O_3 and $MgAl_2O_4$. Obviously, the recrystallization is also acceler-

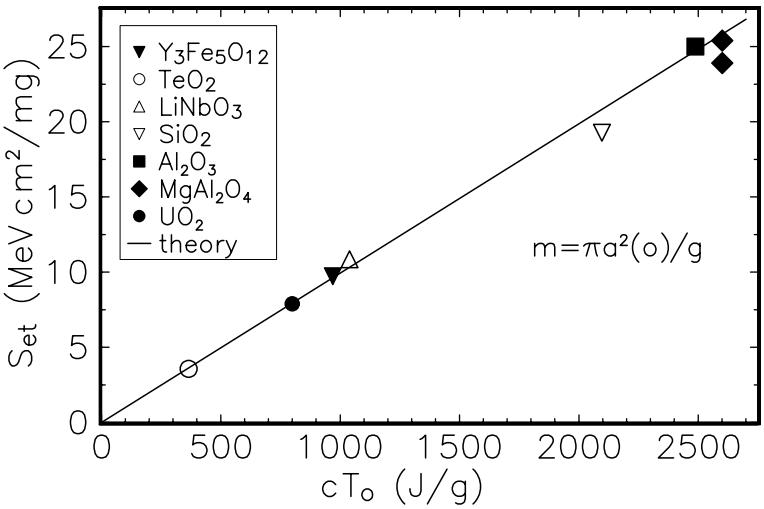

Fig. 3. Threshold of melt formation S_{et} for various solids for irradiation with low velocity ions ($E < 2.2$ MeV/nucleon); c is the average specific heat and $T_o = T_m - T_{ir}$ where T_m is the melting point and T_{ir} is the irradiation temperature. The theoretical line with the slope m is calculated with $a(0) = 4.5$ nm and $g = 0.4$; Al_2O_3, $MgAl_2O_4$, UO_2 present results, others from Ref. [4].

ated at high temperatures. Therefore, in spite of the reduction of S_{et}, a crystal may be amorphizable at room temperature and non-amorphizable at high temperatures.

The experiments of Aruga et al. [17,22] showed that the investigations of the radiation resistance always must include experiments with high fluences, as well, since the study of the properties of single tracks may lead to incorrect predictions when track recrystallization is expected. Experiments in such conditions are highly important since the high fluence is an essential feature of any reactor applications. The above considerations are valid for UO_2 as well. We also emphasize that the predictions based on room temperature studies of ion-induced tracks are not reliable without experiments on the operating temperatures of the nuclear fuel.

We note that it is very advantageous to estimate S_{et} from the position of the amorphous–crystalline boundary since this experiment requires only a single ion beam. The estimate of S_{et} from the track evolution curve requires a number of ion irradiations including beams of heavy ions, as well, if S_{et} is high. On the other hand, the determination of d_{am} is considerably simpler than the accurate measurement of the track diameters.

In Refs. [13,28,34] tracks in $MgAl_2O_4$, UO_2 and Al_2O_3 were discussed theoretically applying the model of Toulemonde et al. [9]. In this model the electron-lattice interaction mean free path λ is the control parameter and S_{et} is deduced by extrapolation of an R_e–S_e curve to $R_e = 0$. A weakness of this procedure is that this model is valid only for $R_e > 3$ nm [3]. Thus the result of the extrapolation is rather doubtful [4]. However, the main difficulty is that the scaling is possible with the $\rho c T_o$ term without the parameters of the model of Toulemonde et al. (see Figs. 2 and 3).

In the model of Toulemonde et al., λ is an adjustable parameter, and ρ, c, T_m and the equilibrium value of the heat of fusion L_m are fixed parameters [11,12]. When L_m is not known (e.g. $LiNbO_3$, $Y_3Fe_5O_{12}$) it is used as a second fitting parameter. Recently, even a new so-called 'cohesion energy criterion' has been proposed for Al_2O_3 and UO_2 and some other insulators: tracks are formed where $T > T_v$ (T_v temperature of vaporization) and the energy corresponding to $L_m + L_v$ (L_v – the latent heat of vaporization) is transferred to the atoms [34]. If this description were correct, one would expect a scaling factor of the form $\rho\ (cT_o + L_m)$ or $\rho\ [c(T_v - T_{ir}) + L_m + L_v]$. The contribution of L_m and L_v is rather high: $L_m/cT_o = 0.3$ for $Y_3Fe_5O_{12}$ and $(L_m + L_v)/cT_o > 2$ for UO_2. The model-independent scaling by $\rho c T_o$ evidences that T_v, L_m, L_v are not relevant parameters for track formation. Obviously, the same is valid for the gap energy of insulators which was also put forward in Ref. [34].

We estimated in Table 1 the room temperature values of S_{et} for some solids, most of which have been proposed for inert matrix applications. The last column is to illustrate the possible effect of ff, where we used the S_e values for I ions of 72 MeV. Our conclusion is that all insulators in Table 1 except MgO may be equally affected by ff.

It is known that tracks are not formed in insulators with predominantly ionic bonds. The origin of this behavior has not been clarified yet. As MgO is an ionic crystal, track formation by ff is not expected. In agreement with this, Aruga et al. did not observe amorphization in MgO after irradiation with 85 MeV I ions up to 1.2×10^{19} ions/m^2 and no step appeared on the irradiated surface. On the other hand, X-ray diffraction measurements revealed a gradual atomic rearrangement in the irradiated polycrystalline samples [17].

Table 1
Threshold electronic stopping power S_{et} for various solids, calculated by Eq. (3)

	ρ (kg/m^3)	c (kJ/K kg)	T_m (K)	S_{et} (keV/nm)	S_{et} (exp) (keV/nm)	S_e/S_{et}
SiC	3210[a]	1.25	3103[a]	Semicond.	–	–
AlN	3310[a]	1.22	3025[a]	Semicond.	–	–
Al_2O_3	3980[a]	1.23	2324[a]	9.8	9.9	1.78
β-Si_3N_4	3210[a]	1.28	2775[a]	10.1	–	1.5
$MgAl_2O_4$	3580[a]	1.23	2408[a]	9.3	9.15, 8.6	1.78
MgO	3580[b]	1.24	3100[c]	Ionic	–	–
CeO_2	7240[d]	0.44	2873[d]	8.2	–	2.20
ZrO_2	5830[f]	0.61	2983[c]	9.5	–	1.95
$ZrSiO_4$	4560[b]	0.82	1960[e]	6.2	–	2.73
UO_2	10960[b]	0.28	3120[c]	8.6	8.66	2.29

For $T_{ir} = 300$ K; ρ – density, c – average specific heat (approximated by the Dulong–Petit rule), T_m – melting point, S_{et} (exp) our estimates from experimental results. In the last column S_e stands for irradiation by 72 MeV iodine ions.

[a] [37].
[b] [38].
[c] [39].
[d] [40].
[e] Incongruent melting [32].
[f] X-ray density [38].

SiC and AlN are semiconductors. While the energy deposition is identical and highly localized in insulators, the initial width of the thermal spike $a(0) > 4.5$ nm is a materials property in semiconductors and it is not a constant. In III–V semiconductors we found that $a(0)$ varied with the gap energy E_g approaching to $a(0) = 4.5$ nm at high E_g values. The efficiency values are also considerably less in semiconductors than in insulators. The changes in the magnitude of the parameters $a(0)$ and g lead to considerably higher values of S_{et}. For example in InSb, the value of S_{et} is about 33 times larger than the estimate according to Eq. (3) for an insulator with identical thermal properties [35]. Thus we do not expect that monoatomic ions can induce tracks in SiC or AlN. Experiments performed on AlN by Zinkle et al. [36] confirm this prediction.

4. Conclusions

The correct S_{et} values can be reliably estimated from the position of the amorphous–crystalline interface in ion irradiation experiments with high fluences. The analysis of ion-induced amorphization data on Al_2O_3, $MgAl_2O_4$ and UO_2 ceramics confirmed the reliability of the predictions of S_{et} based on our thermal spike model. Prediction of the room temperature value of S_{et} for ff energies was made also for β-Si_3N_4, CeO_2, pure ZrO_2, and $ZrSiO_4$. The predicted values of S_{et} are equal within ±10% except $ZrSiO_4$, so in an ideal case (no recrystallization) only minor differences would occur between the track structures. However, the recrystallization processes may lead to considerable differences in a real experiment. According to our present knowledge ff do not induce track damage in SiC, AlN and MgO crystals. In UO_2, $S_{et} = 8.6$ keV/nm is predicted in good agreement with the experiments. For an operating temperature of about 1000° C S_{et} is reduced by about 35–50%. Reliable estimates of radiation resistance require experiments performed at the operating temperatures and with high ion fluences.

Acknowledgment

This work was accomplished with the support of the National Scientific Research Fund (OTKA, Hungary) under contracts No T031756, T043247 and T046990.

References

[1] F. Studer, M. Hervieu, J.M. Costantini, M. Toulemonde, Nucl. Instrum. and Meth. B 122 (1997) 449.
[2] A. Meftah, F. Brisard, J.M. Costantini, M. HageAli, J.P. Stoquert, F. Studer, M. Toulemonde, Phys. Rev. B 48 (1993) 920.
[3] A. Meftah, J.M. Costantini, M. Djebara, N. Khalfaoui, J.P. Stoquert, F. Studer, M. Toulemonde, Nucl. Instrum. and Meth. B 122 (1997) 470.
[4] G. Szenes, F. Pászti, Á. Péter, D. Fink, Nucl. Instrum. and Meth. B 191 (2002) 186.
[5] J. Jensen, A. Dunlop, S. Della-Negra, M. Toulemonde, Nucl. Instrum. and Meth. B 146 (1998) 412.
[6] G. Szenes, Phys. Rev. B 51 (1995) 8026.
[7] G. Szenes, Phys. Rev. B 60 (1999) 3140.
[8] G. Szenes, Appl. Phys. Lett. 81 (2002) 4622.
[9] G. Szenes, Phys. Rev. B 70 (2004) 094106.
[10] G. Szenes, Nucl. Instrum. and Meth. B 191 (2002) 27.
[11] A. Meftah, F. Brisard, J.M. Costantini, E. Dooryhee, M. Hage-Ali, M. Hervieu, J.P. Stoquert, F. Studer, M. Toulemonde, Phys. Rev. B 49 (1994) 12457.
[12] M. Toulemonde, J.M. Costantini, Ch Dufour, A. Meftah, E. Paumier, F. Studer, Nucl. Instrum. and Meth. B 116 (1996) 37.
[13] T. Wiss, Hj Matzke, V.V. Rondinella, T. Sonoda, W. Assmann, M. Toulemonde, C. Trautmann, Prog. Nucl. Energy 38 (2001) 281.
[14] T. Wiss, Hj Matzke, Radiat. Meas. 31 (1999) 507.
[15] S.J. Zinkle, V.A. Skuratov, Nucl. Instrum. and Meth. B 141 (1998) 737.
[16] S.J. Zinkle, H.J. Matzke, V.A. Skuratov, In Microstructural Processes during Irradiation, in: S.J. Zinkle et al. (Eds.), MRS Symp. Proc. Vol. 540, MRS Warrendale, PA, 1999, p. 299.
[17] T. Aruga, Y. Katano, T. Ohmichi, S. Okayasu, Y. Kazumata, S. Jitsukawa, Nucl. Instrum. and Meth. B 197 (2002) 94.
[18] J.F. Ziegler, J.P. Biersack, U. Littmark, The Stopping and Range of Ions in Solids, Pergamon Press, New York, 1985.
[19] B. Canut, S.M.M. Ramos, P. Thevenard, N. Moncoffre, A. Benyagoub, G. Marest, A. Meftah, M. Toulemonde, F. Studer, Nucl. Instrum. and Meth. B 80&81 (1993) 1114.
[20] B. Canut, A. Meftah, N. Moncoffre, S.M.M. Ramos, F. Studer, P. Thevenard, M. Toulemonde, Phys. Rev. B 51 (1995) 12194.
[21] S.M.M. Ramos, N. Bonardi, B. Canut, S. Bouffard, S. Della-Negra, Nucl. Instrum. and Meth. B 143 (1998) 319.
[22] T. Aruga, Y. Katano, T. Ohmichi, S. Okayasu, Y. Kazumata, Nucl. Instrum. and Meth. B 166 (2000) 913.
[23] V.A. Skuratov, S.J. Zinkle, A.E. Efimov, K. Havancsák, Proc. 13th International Conference on Surface Modification of Materials by Ion Beams, 21–26 September 2003, San Antonio, Texas, USA, Surface and Coatings Technology, in press.
[24] G. Szenes, in press.
[25] W. Bolse, B. Schattat, A. Feyh, T. Renz, Nucl. Instrum. and Meth. B 218 (2004) 80.
[26] L. Thome, F. Garrido, Vacuum 63 (2001) 619.
[27] F. Garrido, C. Choffel, L. Thomé, J.C. Dran, L. Nowicki, A. Turos, J. Domagala, Nucl. Instrum. and Meth. B 136–138 (1998) 465.
[28] T. Wiss, Hj Matzke, C. Trautmann, M. Toulemonde, S. Klaumünzer, Nucl. Instrum. and Meth. B 122 (1997) 583.
[29] Hj Matzke, P.G. Lucuta, T. Wiss, Nucl. Instrum. and Meth. B 166 (2000) 920.

[30] T. Sonoda, M. Kinoshita, N. Ishikawa, Y. Chimi, A. Iwase, JAERI-Rev. 29 (2002) 97.
[31] T. Sonoda, M. Kinoshita, N. Ishikawa, Y. Chimi, A. Iwase, JAERI-Rev. 30 (2003) 104.
[32] W.C. Butterman, W.R. Foster, Am. Mineralog. 52 (1967) 880.
[33] L.A. Bursill, G. Braunshausen, Philos. Mag. A 62 (1990) 395.
[34] Ch Dufour, A. Meftah, E. Paumier, Nucl. Instrum. and Meth. B 166&167 (2000) 903.
[35] G. Szenes, Z.E. Horváth, B. Pécz, F. Pászti, L. Tóth, Phys. Rev. B 65 (2002), art. no. 045206.
[36] S.J. Zinkle, J.W. Jones, V.A. Skuratov, Microstructural Processes during Irradiation, in: G.E. Lucas et al. (Eds.), MRS Symp. Proc. MRS, Warrendale, PA, 650 (2001), R3 19.1.
[37] S.J. Zinkle, V.A. Skuratov, D.T. Hoelzer, Nucl. Instrum. and Meth. B 191 (2002) 758.
[38] D.R. Lide, CRC Handbook of Chemistry and Physics, 71st Ed., in chief, CRC, 1990.
[39] H. Kleykamp, J. Nucl. Mater. 275 (1999) 1.
[40] F.S. Galasso, Structure and Properties of Inorganic Solids, Pergamon, New York, 1970.